

Thermal Conductivity and Phonon Scattering by Magnetic Impurities in CdTe

GLEN A. SLACK AND S. GALGINAITIS

General Electric Research Laboratory, Schenectady, New York

(Received 2 August 1963)

Crystals of CdTe containing 1 mole % of Mn, Fe, or ZnTe have been grown from the melt. The segregation coefficients of these impurities and of Co can be understood in terms of differences in the covalent, tetrahedral radii of the various metal atoms. The thermal conductivity, K , of these crystals and of pure CdTe has been measured from 3 to 300°K. A table of K values for pure CdTe is given; its $K=0.075$ W/cm deg at 300°K. The heat transport in pure CdTe is due to phonons, and is limited by phonon scattering by crystal boundaries, isotopes, and other phonons. The local lattice distortions, which are nearly the same for Mn, Fe, and Zn, produce an additional nonmagnetic phonon scattering in the doped crystals. There is also a magnetic scattering, particularly pronounced for the Fe with a $3d^6$ configuration, caused by phonon assisted transitions between various low lying energy levels of the d -shell electrons. The nature and spacing of these levels can be predicted by crystal field theory, and there is qualitative agreement between this theory and the experimental results.

INTRODUCTION

THE study of the thermal conductivity of paramagnetic crystals has been actively pursued for only about 5 years. In this length of time several interesting effects have appeared. In crystals such as MnO,^{1,2} CoF₂,³ Fe₃O₄,⁴ Y₃Fe₅O₁₂,⁵ the concentration of the magnetic ions is quite large, and the thermal conductivity between 3 and 300°K is affected mainly by the cooperative behavior of these ions. In the weakly paramagnetic crystals such as Fe-doped ZnSO₄·7H₂O,⁶ the concentration of magnetic ions is smaller, and the thermal conductivity from 3 to 300°K is affected by these isolated ions acting independently of one another. The present study on doped CdTe is directed at this latter goal of studying weakly paramagnetic crystals. CdTe is a semiconductor,⁷ in contrast to the ionic, essentially electrically nonconducting oxides, halides, and hydrated salts mentioned above. CdTe has a simple, cubic crystal structure, and very pure crystals can be grown.⁸ As will be shown later, crystals can also be grown containing substantial concentrations of elements from the first transition metal series. Thus, CdTe is a good matrix to use for a study of the scattering of phonons by magnetic ions.

PROCEDURE

The plan of the experiment is as follows. First the thermal conductivity K of pure CdTe is measured over the whole temperature range from 3 to 300°K. These results are then analyzed in terms of a theoretical

model which enables one to identify the various phonon-scattering processes in the pure CdTe. The next step is to dope the CdTe with a nonmagnetic cation which has nearly the same mass and size as that of the magnetic cations used later. The K measurements on this doped sample yield a measure of the magnitude of the phonon scattering produced by the localized lattice distortions and the mass fluctuations. Zn-doped CdTe is used for this purpose. The third step is to find several transition metals which can be incorporated into CdTe, e.g., Mn and Fe, and to measure their effect on K . The phonon scattering produced by the Mn and the Fe differ from that of the Zn only because of their magnetic scattering. This extra magnetic scattering is then interpreted in terms of phonon-assisted transitions between various d -shell levels of the magnetic ions. It is found that the magnetic scattering is in reasonable agreement with the predictions from crystal field theory.

SAMPLES

Crystal Chemistry

A knowledge of the crystal chemistry of CdTe and transition metal tellurides is required in order to build the appropriate samples. For example, the most likely nonmagnetic candidates for use with the first-transition metal series are Ca²⁺ and Zn²⁺. Both CdTe and ZnTe have a zinc-blende (cubic ZnS) crystal structure, whereas CaTe has a rocksalt (NaCl) structure. A continuous series of mixed crystals of CdTe-ZnTe can be made, but CaTe will not form such a series. Thus, Zn²⁺ was chosen as the nonmagnetic impurity to be used as a control.

In the transition metal series Ti, V, Cr, Mn, Fe, Co, Ni, Cu, all of the metals, M , form tellurides at or close to the stoichiometric formula MTe . Six of these have the NiAs-type crystal structure, FeTe_{0.95} has the red PbO structure, and CuTe has its own peculiar structure.⁹ In all of these structures the cations have an

¹ G. A. Slack and R. Newman, Phys. Rev. Letters **1**, 359 (1958).

² G. A. Slack, *Proceedings of the International Conference on Semiconductor Physics, Prague, 1960* (Czechoslovakian Academy of Sciences, Prague, 1961 and Academic Press Inc., New York, 1962), p. 630.

³ G. A. Slack, Phys. Rev. **122**, 1451 (1961).

⁴ G. A. Slack, Phys. Rev. **126**, 427 (1962).

⁵ B. Luthi, J. Phys. Chem. Solids **23**, 35 (1962); R. L. Douglas, Phys. Rev. **129**, 1132 (1963).

⁶ H. M. Rosenberg and B. Sujak, Phil. Mag. **5**, 1299 (1960).

⁷ B. Segall, M. R. Lorenz, and R. E. Halsted, Phys. Rev. **129**, 2471 (1963).

⁸ M. R. Lorenz and R. E. Halsted, J. Electrochem. Soc. **110**, 343 (1963).

⁹ R. W. G. Wyckoff, *Crystal Structures* (Interscience Publishers, Inc., New York, 1948-1960).

octahedral environment of anions, whereas Cd in CdTe is in a tetrahedral environment of Te ions. Thus, CdTe will not be able to form a continuous series of mixed crystals with any of the M Te compounds. At best, the M ions will have a finite solubility in CdTe. As long as the solubility of the M ions in CdTe is as large as a few percent, then the phonon scattering in the doped crystals will be sufficient to noticeably lower the thermal conductivity below that of the pure CdTe. Any increase in the phonon scattering caused by the magnetic nature of the M ions will lower K still further.

The estimation of the solubility limit of the M ions in solid CdTe is not very easy. One guide that can be used are the literature references to some studies of the Zn and Cd oxides and sulfides. Another guide is a comparison between the covalent, tetrahedral radii of the M ions and that of Cd. As Kröger¹⁰ has pointed out, a near equality of the radii may be a necessary but is not a sufficient condition for a large solubility. Some cation-cation interactions should also be considered, but will be neglected here for lack of a way to treat them.

In the sulfides Kröger¹⁰ found a large (50 mole %) solubility of β -MnS in CdS at high temperatures, while Schnaase¹¹ found that CdS and β -MnS formed a continuous series of solid solutions at room temperature. The large solid solubility of MnS in CdS is also demonstrated by the data of Medcalf and Fahrig¹² who found a segregation coefficient of $k \sim 1$ for Mn in CdS during the growth of CdS from the melt. Juza *et al.*¹³ have found substantial solubilities of Mn in ZnS, ZnSe, and ZnTe at 600°C. Delves and Lewis¹⁴ have found a large solid solubility of MnTe in HgTe, and found that CdTe-MnTe mixed crystals can be made with up to 75-mole % MnTe.

A table of the tetrahedral radii of various elements is given in the Appendix, and is useful in understanding the formation of mixed crystals. The occurrence of a wide range of miscibility of M Te in CdTe in the solid state is apt to occur if the M -to-Te distance (normalized to a zinc-blende structure) differs by no more than, say, 5% from the Cd-to-Te distance in CdTe. This means the covalent tetrahedral radius of the metal, should lie between 1.35 and 1.63 Å. The $\pm 10\%$ limits would be 1.23 to 1.79 Å. This argument would predict a large miscibility range for Mn in CdTe, a moderate range for Ti, V, Cr, Fe, Ni, Cu, and Zn, and a very small range for Co. Thus, the complete or nearly complete solid solubility of MnS in CdS and MnTe in CdTe can be understood. The ratio of interatomic distances in this sulfide system is 0.96. This ratio is 0.97 for MnTe in CdTe. Crystals of CdTe containing 1 mole % MnTe

were easily grown from the melt by the present authors with only a slight rejection of the Mn from the growing crystal. A crude estimate of the segregation coefficient is $k=0.7$. No attempt was made to grow CdTe crystals with Mn concentrations greater than 1×10^{20} cm⁻³, though this should not be difficult.

The system ZnTe-CdTe was studied by Wooley and Ray,¹⁵ and was found to exhibit a continuous series of solid solutions. Here the interatomic distance ratio is 0.94, and a reasonable range of miscibility might be expected. No difficulty was experienced in the present experiments in growing ZnTe-CdTe mixed crystals from the melt with 1 mole % ZnTe. The value of k is approximately 1. From Fig. 9 in the Appendix one might expect Fe to have about the same solubility as Zn in CdTe. The FeS solubility in natural ZnS crystals has been found¹⁶ to be as high as 44 mole %, while that in synthetic ZnS can be¹⁷ as high as 21 mole %. The FeS content of natural crystals¹⁸ of metacinnabar, HgS, which has the zinc-blende structure, can be as high as 20 mole %. The segregation coefficient for Fe during the growth of HgTe from the melt has been found¹⁹ to be close to 1. In the present experiments a segregation coefficient of 0.3 was found for Fe in melt-grown CdTe. The highest FeTe concentration actually in solid solution obtained in the present CdTe single crystals grown at a rate of 0.5 cm/h was 2 mole %. Higher concentrations could probably be obtained with slower growth rates.

The solubility of Co in CdTe may be quite limited, since the radius of Co is 1.20 Å. This gives a Co-Te distance which is 0.90 of the Cd-Te distance in CdTe. The only mixed-crystal data found in the literature were for CoO in ZnO. Rigamonti²⁰ found that 30-mole % of CoO could be dissolved in ZnO while Robin²¹ found 10-mole %. In the present series of experiments an approximate segregation coefficient of $k=0.1$ was found for Co in CdTe grown from the melt. A crystal containing about 0.01-mole % of CoTe in solid solution was prepared. Most of the Co in that part of the crystal boule which was frozen last appeared as CoTe precipitates with a NiAs-type crystal structure.

Sample Preparation

The single-crystal samples of CdTe used in the present experiment were grown from the melt using the tech-

¹⁵ J. C. Wooley and B. Ray, *J. Phys. Chem. Solids* **13**, 151 (1960).

¹⁶ K. F. Chudoba and M. T. MacKowsky, *Zentr. Mineral. Geol.* **1939A**, 12 (1939).

¹⁷ J. T. S. Van Aswegen and H. Verleger, *Naturwissenschaften* **47**, 131 (1960).

¹⁸ C. Palache, H. Berman, and C. Frondel, *Dana's System of Mineralogy* (John Wiley & Sons, Inc., New York, 1944), 7th ed., Vol. 1, p. 216.

¹⁹ J. Black, S. M. Ku, and H. T. Minden, *J. Electrochem. Soc.* **195**, 723 (1958).

²⁰ R. Rigamonti, *Gazz. Chim. Ital.* **76**, 474 (1946).

²¹ J. Robin, *Compt. Rend.* **235**, 1301 (1952).

¹⁰ F. A. Kröger, *Z. Krist.* **102**, 132 (1939).

¹¹ H. Schnaase, *Z. Physik. Chem.* **29B**, 89 (1933).

¹² W. E. Medcalf and R. H. Fahrig, *J. Electrochem. Soc.* **105**, 719 (1958).

¹³ R. Juza, A. Rabenau, and G. Pascher, *Z. Anorg. Allegem. Chem.* **285**, 61 (1956).

¹⁴ R. T. Delves and B. Lewis, *J. Phys. Chem. Solids* **24**, 549 (1963).

TABLE I. Properties of the CdTe samples.

Sample run number	L^a cm	D^b cm	Purity	Comments
R-69	2.0	0.50	Pure	As-grown
R-70	2.0	0.46	$1.70 \times 10^{20} \text{ cm}^{-3}$ Fe	As-grown
R-71	1.9	0.42	$1.28 \times 10^{20} \text{ cm}^{-3}$ Mn	As-grown
R-72	2.1	0.51	$1.4 \times 10^{20} \text{ cm}^{-3}$ Zn	As-grown
R-73	0.8	0.29	$1.64 \times 10^{20} \text{ cm}^{-3}$ Fe	As-grown
R-85	2.0	0.50	Pure	Sample R-69 after argon firing
R-87	0.8	0.29	$1.64 \times 10^{20} \text{ cm}^{-3}$ Fe	Sample R-73 after argon firing
R-93	1.1	0.28	Pure	Cd fired after growing
R-94	1.0	0.29	$1.28 \times 10^{20} \text{ cm}^{-3}$ Mn	Part of R-71 after Cd firing
R-95	0.8	0.25	$1.1 \times 10^{20} \text{ cm}^{-3}$ Zn	Part of R-72 after Cd firing
R-96	0.9	0.24	Very Pure	As-grown

^a L = length of sample.

^b D = average diameter of sample.

nique described by Heumann.^{8,22} The growth rate was about 0.5 cm/h. Sealed crucibles of fused quartz coated with pyrolytic graphite were employed.

All of the crystals except R-93 and R-96 were grown by the authors using 99.999% tellurium²³ and 99.999% cadmium²⁴ as starting material. The crystals were grown directly from the melt after the starting materials were reacted. No zone purification of the CdTe was attempted. Samples R-93 and R-96 were grown by Lorenz⁹ from purer CdTe which was subsequently zone purified. Sample R-96 was made from especially pure CdTe which had been zoned 30 times before growing.

The boules, as grown, contained some small number of twin boundaries. CdTe twins readily along (111) planes. A small number of these twin boundaries, say 10 per cm, along the length of the sample will not affect the thermal conductivity very much because there is very little strain in, or distortion of, the crystal lattice at a twin boundary. These samples, listed in Table I, contained 1 to 10 twin boundaries per cm and were not, crystallographically speaking, single crystals. The samples were in the shape of rods of length, L , and had a nearly square cross-sectional area A . The effective diameter, D , in Table I is computed from $(\pi D^2/4) = A$.

Three types of tests were made in order to determine the impurity content. First crystals R-69, R-70, R-71, R-93, and R-96 were analyzed with an emission spectrograph and a list of trace impurities was compiled. These crystals were checked for 28 different metallic impurities. Special attention was paid to the first transition metal series from Ca to Zn. Of these, there were 25 foreign or unintentional impurities including Mn, Fe,

and Zn which had concentrations $< 10^{18} \text{ cm}^{-3}$. The three impurities, Be, Li, and Si, with concentrations $> 10^{18} \text{ cm}^{-3}$, are listed in Table II. Of the 25 there were 12 elements including Mn, Co, Ni, and Cu, whose concentrations were $< 10^{17} \text{ cm}^{-3}$. In order to obtain some information about nonmetallic impurities a mass spectrometer analysis was run on the very purest sample, R-96. There were measurable traces of many elements including carbon, hydrogen, oxygen, sulfur, selenium, zinc, etc. No results were obtained for silicon. The most abundant impurity found by this method in R-96 was carbon at a concentration of $5 \times 10^{17} \text{ cm}^{-3}$. The next most abundant was $5 \times 10^{16} \text{ cm}^{-3}$ of oxygen. This crystal and all the others were grown in fused silica tubes which had been internally coated with pyrolytic graphite. This coating is probably the source of the carbon. Table II shows the most abundant impurities found in these analyses. The Fe-doped sample, R-70, shows some enhanced pickup of Si from the quartz tube. The Si concentration is only 3% of that of the Fe, and should have very little effect on K compared to the effect of the Fe. The Mn-doped sample, R-71, in Table II shows a trace of Si and some Be from an unknown source. Again Mn is the dominant impurity in R-71. The undoped samples R-69, R-93, R-96 are much purer.

In the third tests the concentrations of the Mn, Fe, or Zn in the doped crystals were determined by wet chemistry methods as outlined in a general way by Willard and Diehl.²⁵ Some special procedures were necessary to eliminate the Cd and Te from the solutions before titration. The accuracies of the determinations are $\pm 0.03 \times 10^{20} \text{ cm}^{-3}$ for Mn and Fe and $\pm 0.1 \times 10^{20} \text{ cm}^{-3}$ for the Zn. For the present purposes the concentrations of the Mn, Fe, or Zn in the as-grown, doped samples of CdTe are equal, and amount to a replacement of 1.1% of the Cd atoms by the impurity atoms.

The chemical composition of CdTe is a question of not only what foreign atoms are present, but also of the stoichiometry,²⁶ i.e., the Cd to Te ratio. Deviations from

 TABLE II. Impurity content of several CdTe samples in atoms/cm³.

Element	Sample				
	R-96	R-93	R-69	R-70	R-71
Be	$< 4 \times 10^{17}$...	$< 4 \times 10^{17}$	$< 4 \times 10^{17}$	4×10^{18}
C	5×10^{17a}
Ca	6×10^{16a}	...	$< 9 \times 10^{16}$	1×10^{18}	$< 9 \times 10^{17}$
Fe	$< 1 \times 10^{17}$	1×10^{17}	2×10^{17}	high ^b	$< 6 \times 10^{17}$
Li	$< 1 \times 10^{18}$...	$< 1 \times 10^{18}$	$< 1 \times 10^{18}$	2×10^{18}
Mg	$< 6 \times 10^{16a}$...	$< 1 \times 10^{17}$	1×10^{18}	$< 1 \times 10^{18}$
Mn	$< 6 \times 10^{16}$...	$< 6 \times 10^{16}$	$< 6 \times 10^{16}$	high ^b
Si	$< 3 \times 10^{17}$	4×10^{17}	3×10^{17}	5×10^{18}	1×10^{18}
Zn	2×10^{16a}	...	$< 5 \times 10^{17}$	$< 5 \times 10^{16}$	$< 3 \times 10^{18}$

^a Determined with a mass spectrometer. The other values have been determined by emission spectrography.

^b High—means the sample has been intentionally doped with this element. See Table I.

²² F. K. Heumann, J. Electrochem. Soc. **109**, 345 (1962).

²³ From American Smelting and Refining Company, Central Research Laboratory, South Plainfield, New Jersey.

²⁴ From Cominco Products, Inc., 933 West 3rd Avenue, Spokane, Washington.

²⁵ H. H. Willard and H. Diehl, *Advanced Quantitative Analysis* (D. Van Nostrand Company, Inc., New York, 1943).

²⁶ J. S. Prener, *Advan. Chem.* **39**, 170 (1963).

a 1:1 stoichiometric ratio may produce vacancies, interstitials, clusters, or precipitate phases in the samples. There is some evidence for the presence of such stoichiometric deviations in²⁷ CdTe which produce vacancies or interstitials. In the related ZnTe excess Te appears²⁸ to produce Te precipitates. In HgTe about 2 mole % of excess Te in solid solution at 450°C is reported.¹⁴ There is substantial evidence that both vacancies²⁹ and precipitates^{30,31} can produce significant phonon scattering at low temperatures. Hence, some effort was made to control the stoichiometry of the present CdTe samples. Some samples were measured in the as-grown condition, others were heat treated, see Table I. Sample R-96 was grown from the purest starting material, and was carefully controlled to be as near to a stoichiometric 1:1 ratio as possible. Its K is the highest at all temperatures of any of the samples studied. The other as-grown samples may have a slight excess of Te. Three samples, R-93, R-94, R-95, were heat-treated in Cd vapor at 900°C in order to equilibrate them at the Cd-rich side of the possible solid solution range.^{32,33} This heat treatment or firing was carried out in sealed fused silica tubes which had been internally coated with pyrolytic graphite. The crystal samples and a few milligrams of excess Cd were placed in this evacuated tube and heated at 900°C for some hours. Samples R-94 and R-95 were treated for 5 h, sample R-93 was given a long-time treatment³³ of 170 h. All three samples were rapidly cooled to room temperature by removing the silica tubes from the furnace and allowing them to cool in air. Sample R-95 suffered some loss of Zn, which is quite volatile during this heat-treatment process. The numbers in Table I show that about 23% of the original Zn was lost. Sample R-94, which was doped with the much less volatile Mn, showed little, if any, loss of Mn.

For a comparison, samples R-85 and R-87 were heat treated in an argon atmosphere at $1\frac{1}{2}$ atm pressure in similar fused silica tubes for 1 h at 900°C. These tubes were quenched rapidly to room temperature in an oil bath. This heat treatment in argon will tend to drive the stoichiometry of the crystals toward the Te rich side of the solid solution range because Cd preferentially evaporates from them. Unfortunately, no crystals were heat treated just at the Te-rich solid-solution boundary by adding excess Te to the fused silica tubes.

The x-ray lattice constants of several samples were also measured at 298°K. The pure CdTe, R-69, had a value of 6.481 Å, which agrees with Wooley and Ray.¹⁵

²⁷ D. deNobel, Philips Res. Rept. **14**, 430 (1959).

²⁸ R. T. Lynch, D. G. Thomas, and R. E. Dietz, J. Appl. Phys. **34**, 706 (1963).

²⁹ R. O. Pohl, Phys. Rev. **118**, 1499 (1960).

³⁰ G. A. Slack, Phys. Rev. **105**, 832 (1957).

³¹ J. M. Worlock, Ph.D. thesis, Cornell University, Ithaca, New York, 1962 (unpublished).

³² M. R. Lorenz, J. Phys. Chem. Solids **23**, 939 (1962).

³³ M. R. Lorenz and H. H. Woodbury, Phys. Rev. Letters **10**, 215 (1963).

TABLE III. Representative thermal conductivity values for pure CdTe.

T °K	K W/cm deg	T °K	K W/cm deg
0	0.0	65	0.57
10	5.0	80	0.44
15	3.4	100	0.31
20	2.63	150	0.184
30	1.80	200	0.127
40	1.17	250	0.095
50	0.84	300	0.075

The lattice constants of the Mn-, Fe-, and Zn-doped samples were slightly less (0.001 to 0.002 Å), but these differences are of the order of the experimental uncertainty.

The electrical properties of the various crystals grown by the authors have not yet been measured. However, there are some data on samples R-93 and R-96, obtained from Lorenz.^{7,33} Sample R-93 is from the same parent crystal as sample C in Ref. 32, and its electrical properties are the same as those given for C in this reference. The highest purity sample, R-96, is n type and very high electrical mobility at low temperatures. Its electrical parameters are very similar to Sample A in Ref. 7.

EXPERIMENTAL TECHNIQUE

The thermal conductivity was measured from 3 to 300°K by a steady-state technique³ employing gold-cobalt versus manganin thermocouples. In order to obtain accurate values for the thermal conductivity of pure CdTe, the K was first measured from 100 to 300°K using a close fitting thermal-radiation shield³ which had a longitudinal temperature distribution identical to that of the sample. The best value of K for pure CdTe, sample R-96, at 300°K is $K=0.075\pm 0.003$ W/cm deg. The radiation shield was not used in any other runs. Thus, the K values at 300°K measured without the shield were higher by about 0.005 W/cm deg. than the true values because of thermal-radiation losses from the sample heater. At temperatures below 200°K the radiation losses are negligible.

EXPERIMENTAL RESULTS

The K versus T data for the samples R-69, R-93, and R-96 of high-purity CdTe are shown in Fig. 1. The relative accuracy of the various data points is about $\pm 2\%$. The absolute accuracy of any given K value is about $\pm 5\%$. The absolute temperatures have been measured to an accuracy of better than $\pm 1\%$. It is felt that the results for the as-grown sample R-96 are sufficiently representative of high-purity CdTe so that smoothed values of K versus T are given in Table III. The values below 10°K will depend upon sample size, and are therefore not given. The maximum K observed for R-96 was 6.5 W/cm deg at 6.5°K. The pronounced

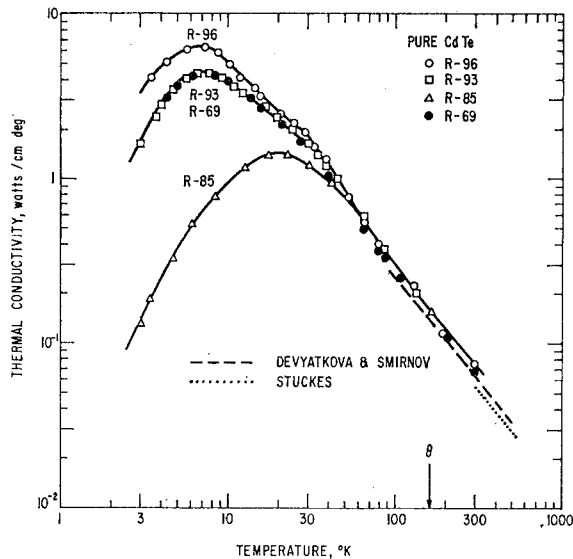


FIG. 1. The thermal conductivity versus temperature for three different crystals of pure CdTe. The Debye temperature is θ . Some previous data of Devyatkova and Smirnov, and of Stukes are shown for comparison.

change in slope at 30°K is believed to be real, and is not an instrumental error. The slope of the K versus T curve for $R-96$ changes from $K \sim T^{0.95}$ just below 30°K to $K \sim T^{1.50}$ just above 30°K. A short experiment was performed in order to determine whether photo excitation at low temperatures would influence this "kink" at 30°K. A small incandescent lamp was mounted inside the cryostat and the sample, $R-93$, was illuminated for 1 to 3 min at several temperatures between 4 and 30°K. The production of hole-electron pairs by this technique has led to large changes in the electrical properties on this sample.³³ However, the K values of the crystal were in no way changed by the illumination. Some small transient heating of the thermocouples was, of course, observed when the light was turned on. The "kink" in the K versus T curve is not associated with changes in the electrical behavior of the CdTe crystals or the number of charge carriers present.

Some other data on the K of reasonably pure CdTe are available from the literature. Holland³⁴ has measured one CdTe sample from 1.7 to 300°K and his results are in very good agreement with sample $R-69$. Devyatkova and Smirnov³⁵ have measured crystals of CdTe from 90 to 470°K, and their results are given in Fig. 1. Their values are about 15% less than those found in the present experiment. Stuckes^{36,37} *et al.* have published

³⁴ M. G. Holland, *Bull. Am. Phys. Soc.* 8, 15 (1963).

³⁵ E. D. Devyatkova and I. A. Smirnov, *Fiz. Tverd. Tela* 4, 2507 (1962) [translation; *Soviet Phys.—Solid State* 4, 1836 (1963)].

³⁶ A. D. Stuckes, *Brit. J. Appl. Phys.* 12, 675 (1961).

³⁷ R. P. Chasmar, E. W. Durham, and A. D. Stuckes, *Proceedings of the International Conference on Semiconductor Physics, Prague, 1960* (Czechoslovakian Academy of Sciences, Prague, 1961 and Academic Press Inc., New York, 1962), p. 1018.

values for CdTe in the temperature range from 310 to 530°K. These values for undoped CdTe are also shown in Fig. 1, and are approximately 25% smaller than those for $R-96$. Stuckes' values were obtained by a comparative method instead of an absolute method, which was used in the present experiments. Ioffe and Ioffe³⁸ have given some K values for polycrystalline CdTe at 300°K. A representative value is 0.052 W/cm deg., about 30% smaller than that found for $R-96$. The agreement of the present data with these previous results is satisfactory. The present values of K are higher, and indicate high purity and/or more nearly perfect crystals than were studied before.

The experimental run $R-85$ was a remeasurement of the same sample used for $R-69$ with a diameter of 0.50 cm. The large decrease in K in the region between 3 and 30°K was produced as a result of the heat treatment in argon at 900°C. The source of the extra phonon scattering in $R-85$ compared to $R-69$ is not known. It may be caused by dislocations generated during the rapid quenching, by lattice vacancies, by interstitial Te, or by small size Te precipitates, or by something else. Somewhat similar rapid cooling of the Cd-fired samples did not noticeably reduce K . Thus, dislocations produced by thermal stress are probably ruled out. In view of the probable excess Te in the sample, the authors are inclined to believe that Te precipitates in $R-85$ are the cause of the reduction in K . The main conclusion to be drawn from the K of $R-85$ is that this heat treatment did not reduce the K to values anywhere near as low as those found for the Fe-doped samples $R-70$ and $R-73$.

The results for the as-grown, doped CdTe samples

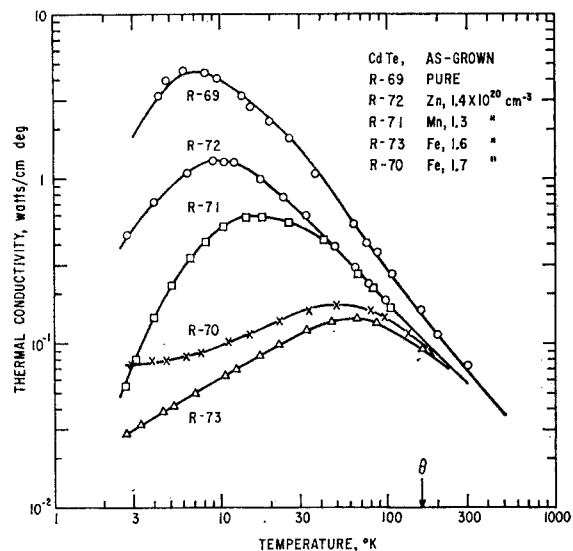


FIG. 2. The thermal conductivity versus temperature for both pure and doped CdTe containing about 1 mole % impurity. These crystals were measured in the as-grown state before any heat treatment. The Debye temperature is θ .

³⁸ I. V. Ioffe and A. F. Ioffe, *Fiz. Tverd. Tela* 2, 781 (1960) [translation: *Soviet Phys.—Solid State* 2, 719 (1960)].

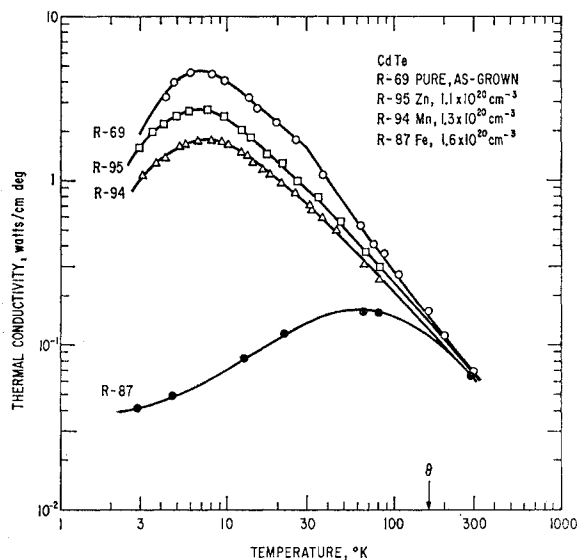


FIG. 3. The thermal conductivity versus temperature for pure, as-grown CdTe, *R-69*, and for three doped, heat-treated samples, *R-87*, *R-94*, *R-95*.

are shown in Fig. 2. The K values all lie below those for pure CdTe, and the amount of reduction in K is generally larger at the lower temperatures. The results for *R-69* are used for pure CdTe since it was made from the same CdTe that was used as the starting material for *R-70*, *R-71*, and *R-73*. There are some other data in the literature on the K of doped CdTe. Chasmar *et al.*³⁷ have measured a sample containing 10^{18} cm⁻³ of iodine from 310 to 500°K. They also measured CdTe with 50 mole % and 80 mole % HgTe at room temperature. Ioffe and Ioffe³⁸ have made room-temperature K measurements on polycrystalline samples containing Zn and Se. Just for comparison with CdTe there are also some measurements between 77 and 300°K on HgTe doped with CdTe which have been reported by Blair.³⁹ In these several studies only nonmagnetic impurities were used, and the results can be explained on the same basis that will be employed later for the Zn-doped CdTe.

The results for the heat-treated and doped samples, *R-87*, *R-94*, *R-95* are shown in Fig. 3. The curve for the Zn-doped sample, *R-95* is for a Zn concentration of 1.1×10^{20} cm⁻³, see Table I. Again the as-grown, undoped sample, *R-69*, is used as the comparison. The main feature to notice is that the Cd firing of the Mn-doped sample, *R-94*, has raised the K in the 3 to 40°K range, but has not changed it appreciably at higher temperatures. At 3°K the increase is a factor of 12 compared to *R-71* in Fig. 2. The same general behavior is seen for the Zn-doped sample, *R-95*, where an increase in K at 3°K of 3 times has occurred compared to *R-72* in Fig. 2. The Cd firing appears to eliminate some source of phonon scattering such as excess Te in the as-grown

³⁹ J. Blair, *Bull. Am. Phys. Soc.* 5, 164 (1960).

samples. Crystal *R-87* was heat-treated in argon in an attempt to further decrease its K by the possible introduction of excess Te. The K curve for *R-87* is substantially the same as that for *R-73*, its parent. This heat treatment had very little effect. Sample *R-87* broke before it could be heat treated in Cd. Such a treatment might have raised the K of *R-87* (i.e., *R-73*) so that it would nearly coincide with the K of *R-70*, see Fig. 2. However, the phonon scattering produced by the Fe is so large that the changes caused by shifts in stoichiometry such as seen in *R-72*, *R-85*, *R-87*, *R-95*, would produce at most a 30% change in the observed K of *R-70* or *R-73* at 3°K. The effect at 10°K and above would be considerably less.

In summary it is believed that the K of pure CdTe is given by *R-96* in Fig. 1, CdTe doped with 1.28×10^{20} cm⁻³ Mn by *R-94* in Fig. 3, CdTe doped with 1.7×10^{20} cm⁻³ Fe by *R-70* in Fig. 2. and CdTe doped with 1.4×10^{20} cm⁻³ Zn by the dotted curve in Fig. 4. This curve for a Zn-doped sample is a composite of the results from *R-72* and *R-95*. These four K curves, redrawn in Fig. 4, represent samples in which there is very little, if any, extra phonon scattering produced by deviations from stoichiometry. The samples prepared at 900°C at the Cd-rich solid-solution boundary of CdTe appear to possess very few defects that can scatter phonons. On this basis these samples may have a Cd-to-Te ratio that is very nearly 1-to-1. The samples prepared toward the Te-rich boundary possess some defects, perhaps Te precipitates, which scatter phonons. The next question is how to explain the curves in Fig. 4 from a theoretical standpoint.

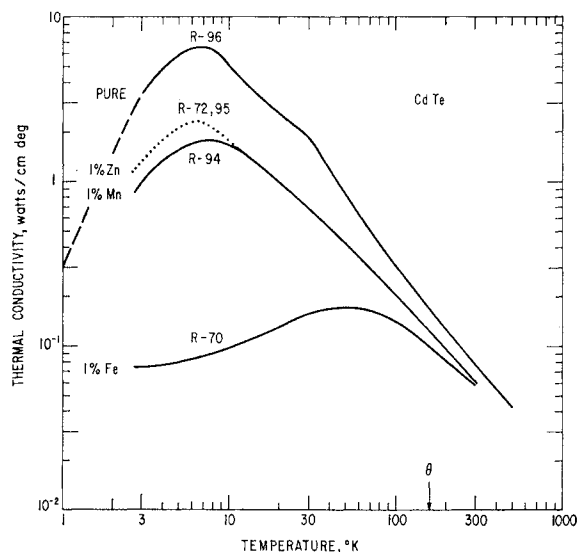


FIG. 4. A summary of thermal conductivity results on nearly stoichiometric CdTe crystals. The purest CdTe sample, *R-96*, is compared with the other sample in which about 1% of the Cd has been replaced by Zn, Mn, or Fe. The dotted curve labeled *R-72, 95* is a composite of the results for *R-72* and *R-95* adjusted to a Zn concentration of 1.4×10^{20} cm⁻³.

COMPARISON WITH THEORY

The interpretation of the above results is based on the predictions of a simplified theoretical model. The expected behavior of the thermal conductivity versus temperature of the pure and the Zn-doped CdTe can be estimated. The theory that will be used here is based on the assumptions that (1) phonons transport all of the heat, (2) the phonons can be represented by a Debye-type approximation with a single-frequency-independent phonon velocity and a maximum phonon frequency fixed by the Debye temperature, (3) the appropriate relaxation times for the various phonon-scattering mechanisms are known. With this basis the thermal conductivity can be calculated by evaluating some definite integrals. This procedure has been used by Klemens,⁴⁰ Slack,⁴¹ Callaway,⁴²⁻⁴⁴ and others. The treatment used here will closely follow that used by Callaway. The phonon-scattering mechanisms that will be considered are other phonons, isotopes, nonmagnetic point impurities, magnetic point impurities, and crystal boundaries.

Umklapp Processes

At temperatures in the region of $T \geq 0.1\theta$ the dominant phonon-scattering mechanism is umklapp scattering by other phonons. The Debye temperature θ at $T=0^\circ\text{K}$ for CdTe has been computed from the elastic constants, see Table IV. Since $\theta=158^\circ\text{K}$ for CdTe this temperature region $T \geq 0.1\theta$ is important in the present study. No good theoretical calculation of the umklapp-scattering relaxation time τ_u for all temperatures has yet been made.⁴⁵ However, the thermal conductivity of several high purity, isotopically clean crystals has been meas-

TABLE IV. Physical properties of CdTe.

Crystal structure = zinc-blende lattice
a_0 = lattice constant = 6.481 Å
ρ = crystal density = 5.852 gm/cm ³
V_0 = average volume per atom = 34.04 (Å) ³
M = average g-atomic mass per atom = 120.0g
γ = assumed Gruneisen's constant = 2
c_{ij} = elastic constant
$c_{11} = 5.351 \times 10^{11}$ dyn/cm ² at 25°C
$c_{12} = 3.681 \times 10^{11}$ dyn/cm ² at 25°C
$c_{44} = 1.994 \times 10^{11}$ dyn/cm ² at 25°C
θ = Debye temperature at 0°K = 158°K
v = average sound velocity = 2.0×10^6 cm/sec
Γ = point-defect scattering parameter
$\Gamma(\text{Zn}) = 4.95 \times 10^{-5}$
$\Gamma(\text{Cd}) = 2.25 \times 10^{-5}$
$\Gamma(\text{Te}) = 2.34 \times 10^{-5}$
$\Gamma(\text{CdTe}) = 2.31 \times 10^{-5}$
$\Gamma(\text{Zn}_{0.01}\text{Cd}_{0.99}\text{Te}) = 9.37 \times 10^{-5}$

⁴⁰ P. G. Klemens in *Solid State Physics*, edited by F. Seitz and D. Turnbull (Academic Press Inc., New York, 1958), Vol. 7, p. 1.

⁴¹ G. A. Slack, *Phys. Rev.* **105**, 832 (1957).

⁴² J. Callaway, *Phys. Rev.* **113**, 1046 (1959).

⁴³ J. Callaway and H. C. von Baeyer, *Phys. Rev.* **120**, 1149 (1960).

⁴⁴ J. Callaway, *Phys. Rev.* **122**, 787 (1961).

⁴⁵ P. Carruthers, *Rev. Mod. Phys.* **33**, 92 (1961).

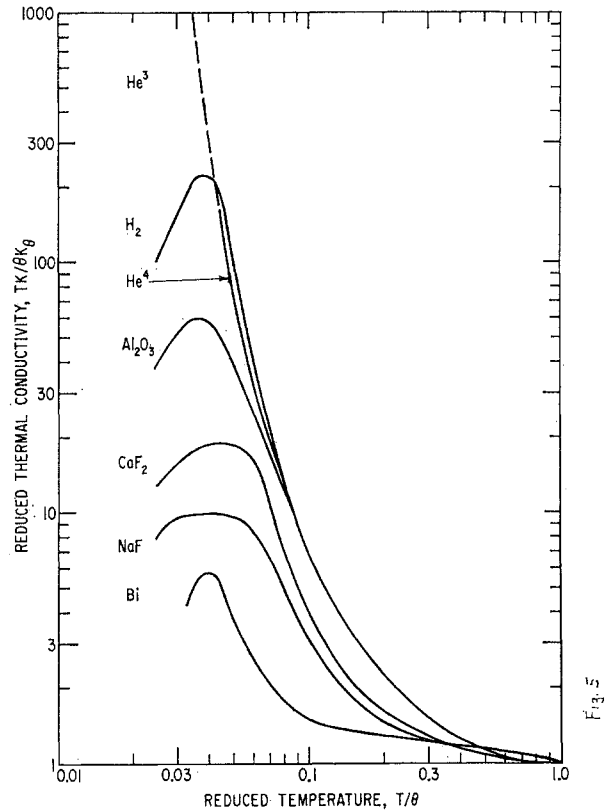


FIG. 5. The reduced thermal conductivity, $TK/\theta K_\theta$, versus reduced temperature, T/θ , for seven nearly or completely isotopically pure solids. The various symbols θ , K_θ , etc. are explained in the text.

ured, and the results for $T \geq 0.1\theta$ can be approximated by a "universal" curve.^{3,46} This "universal" curve is the ratio of K at temperature T to K_θ , the value of K at $T=\theta$, and is assumed to depend only on the reduced temperature (T/θ).

$$K/K_\theta = \text{function}(T/\theta). \tag{1}$$

This assumption is founded on about the same basis as those used to derive the Debye specific-heat function $C_v(T/\theta)$. Figure 5 shows a plot of $TK/\theta K_\theta$ versus T/θ for the monoisotopic (or nearly so) solids He^3 , H_2 , He^4 , Al_2O_3 , CaF_2 , NaF , and Bi . The new NaF data are from Walker⁴⁷ using $\theta=430^\circ\text{K}$, the rest are from Slack.³ The largest value of K/K_θ that occurs in Fig. 3 at a particular T/θ value has been chosen as a point on this "universal curve" denoted by $f(T/\theta)$. If only umklapp scattering is present, then the thermal conductivity is given by Eq. (1) of Ref. 42 with the normal phonon scattering process relaxation time τ_n set at infinity and the combined relaxation time τ_c set equal to the umklapp relaxation, τ_u . The theoretical value of the

⁴⁶ G. Leibfried and E. Schlömann, *Nachr. Akad. Wiss. Goettingen, Math.-Physik. Kl.* **4**, 71 (1954).

⁴⁷ C. T. Walker, *Bull. Am. Phys. Soc.* **8**, 207 (1963).

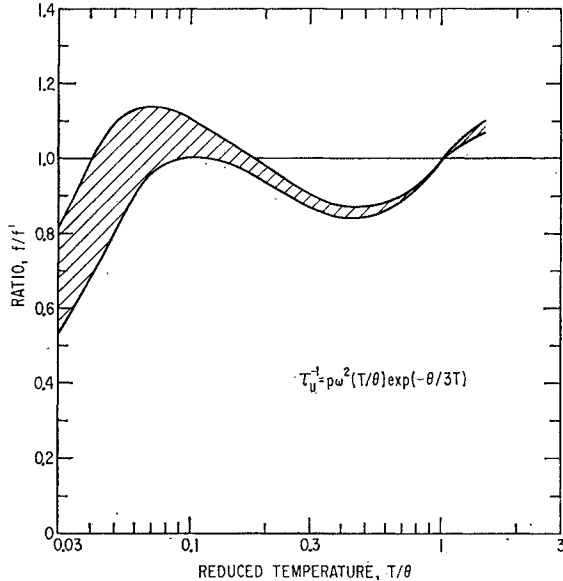


FIG. 6. The ratio between the observed thermal conductivity function f and the computed function f' versus reduced temperature. The computed f' is based on a relaxation time τ_u for phonon scattering by umklapp processes which is substituted into Eq. (2).

thermal conductivity, K' , denoted by the prime, is

$$K'(T) = \frac{k}{2\pi^2 v} \left(\frac{kT}{\hbar} \right)^3 \int_0^{\theta/T} \tau_c \frac{x^4 e^x dx}{(e^x - 1)^2}, \quad (2)$$

where k = Boltzmann's constant, T = absolute temperature, v = average sound velocity, \hbar = Planck's constant, θ = Debye temperature, $x = (\hbar\omega/kT)$, and ω = phonon frequency in radians per second. It has been found that a useful expression for τ_u in Eq. (2) is:

$$(\tau_u)^{-1} = p\omega^2(T/\theta)\exp(-\theta/bT). \quad (3)$$

There are two adjustable constants, p and b . The experimentally determined $f(T/\theta)$ can be fitted quite well in the range $0.05\theta \leq T \leq 2\theta$ with $b = 3.00$. Such a value of b is quite reasonable.^{3,46} The value of p is fixed by the observed value of K'_θ for a particular crystal. The match between the experimentally determined $f(T/\theta)$ and the theoretically calculated $f'(T/\theta) = K'/K'_\theta$ computed from Eq. (2) and (3) is shown in Fig. 6 where f/f' has been plotted versus (T/θ) . The width of the curve is caused by the uncertainty in the experimental value of $f(T/\theta)$. The maximum disagreement between the observed and computed values is $\pm 20\%$ for $0.05\theta \leq T \leq 2\theta$. Over this temperature range f changes by a factor of 4000. Such agreement is interesting even if fortuitous.

An approximate value of p can be obtained from an estimated K'_θ given by Leibfried and Schlömann⁴⁶ in their Eq. (38). Combining their K'_θ with the present Eq. (2) and (3) gives

$$p = O(1)\hbar\gamma^2 m_a^{-1} v^{-2}, \quad (4)$$

where $O(1)$ is a constant which turns out to be equal to unity within $\pm 20\%$, γ = Grüneisen's constant, and m_a = average mass of a single atom in the solid. For CdTe Eq. (4) yields $p = 5.8 \times 10^{-16} \text{ sec}^{-1}$ if $\gamma = 2.0$. The best experimental fit to the measured value of K'_θ gives $p = 7.0 \times 10^{-16} \text{ sec}^{-1}$. This agreement is satisfactory. Thus, this empirical fitting procedure gives an expression for τ_u from Eq. (3) and (4) of

$$(\tau_u)^{-1} \sim \frac{\hbar\gamma^2\omega^2 T}{m_a v^2 \theta} \exp\left(\frac{-\theta}{3T}\right), \quad (5)$$

which can be applied to solids other than CdTe. At a temperature of $T = \theta$ for phonons at the maximum frequency $\hbar\omega = k\theta$, the umklapp relaxation time is $\tau_u = 6 \times 10^{-12} \text{ sec}$ for CdTe. This is equivalent to a relaxation distance, $v\tau_u$, of 120 Å. This distance is a reasonable value for umklapp process scattering for temperatures near $T = \theta$.

Since the τ_u expression in Eq. (3) is only empirical, it is worthwhile to consider some possible variants of it. Equation (3) can be rewritten as

$$(\tau_u)^{-1} \sim \omega^\alpha (T/\theta)^\beta \exp(-\theta/bT),$$

with $\alpha = 2$, $\beta = 1$, and $b = 3$. The temperature dependence of K' from Eq. (2) is determined by the integers α and β , and the constant b . The basic limitations on b , α , and β are $b \geq 1$ for umklapp processes⁴⁶ and $\alpha \leq 2$ in order for the integral in Eq. (2) to be finite. The temperature dependence of K' from Eq. (2) in the region $T \geq \theta$ is insensitive to α and b but depends strongly on β . In order that K' vary as T^{-1} for $T \geq \theta$ it is necessary that $\beta = 1$. In the low-temperature region $T < \theta$ the K' curve is determined by both b and α , but is insensitive to β . A good fit to the $f(T/\theta)$ curve has been obtained in Fig. 6 for the choice $\alpha = 2$, $\beta = 1$, $b = 3.0$. The $f(T/\theta)$ curve can also be fitted, though considerably less well, by using $\alpha = 1$, $\beta = 1$, and $b = 2$ to 2.5. The expression for τ_u^{-1} proposed by Klemens⁴⁸ for $T \ll \theta$ uses $\alpha = 1$ and $\beta = -1$, and clearly will not work near $T = \theta$ in Eq. (2). Both Pohl⁴⁹ and Agrawal and Verma⁵⁰ have used $\alpha = 2$, $\beta = 3$. Pohl uses $b \sim 14$ for LiF and Agrawal and Verma use $b = 2.4$ for solid He⁴ for $T \ll \theta$.

Normal Processes

One intrinsic scattering process has been neglected so far, normal phonon scattering. In the theory developed by Callaway⁴²⁻⁴⁴ these processes have been included. If the ratio $s(T) = (\tau_n/\tau_u)$ is, as Callaway assumes, a function of temperature only and not of the phonon-frequency ω , then Eq. (16) of Ref. 44 can be written as

$$K'_{un} = K'_u \left[\frac{s + J_4^2/J_2 J_6}{s + 1} \right], \quad (5)$$

⁴⁸ See Ref. 40, p. 50.

⁴⁹ R. O. Pohl, Phys. Rev. **118**, 1499 (1960).

⁵⁰ B. K. Agrawal and G. S. Verma, Phys. Rev. **128**, 603 (1962).

where K'_u is the thermal conductivity computed assuming only umklapp processes are important, and K'_{un} is that computed when both are important. The integrals $J_r(\theta/T)$ have been computed by MacDonald and Towle⁵¹ for $r=2,3,4,6$. The ratio $(J_4)^2/J_2J_6$ varies from $(7/25)$ at $T=0$ to $(5/9)$ at $T=\infty$. For $T \ll \theta$ the umklapp processes are very infrequent compared to normal processes, so that $s=0$ at $T=0$. For $T \geq \theta$ the normal and umklapp processes should be almost equally probable to within an order of magnitude.⁵² Hence, for $T \geq \theta$ the range of s is $10 > s > 0.1$. Thus, the [] expression in Eq. (5) and hence K'_{un}/K'_u varies from 0.28 at $T=0$ to a maximum of 1 at $T=\infty$. The conclusion, based on Callaway's Debye-type model, is that $f'(T/\theta)$ is not very sensitive to τ_n and depends mainly on τ_u . In fact τ_n and hence s can be set equal to ∞ without any appreciable error. This is just what was done in determining the empirical Eq. (3) for τ_u .

Pure CdTe

Even though there is some uncertainty in using the empirically derived Eq. (3) for τ_u in CdTe in those cases where other scattering processes are also important, we shall now do just this. The justification is essentially that Eq. (3) appears to give a better fit to $f(T/\theta)$ over a wider temperature range than those equations used previously by other authors. In pure CdTe we will need to combine τ_u with the relaxation times for crystal boundary scattering τ_b and isotope scattering τ_i . The quantities τ_b and τ_i are known on reasonably good theoretical grounds.^{40,53} These are

$$\tau_b^{-1} = v/L \text{ and } \tau_i^{-1} = A\omega^4, \quad (6)$$

where $A = (3V_0\Gamma/\pi v^3)$, L = crystal diameter, V_0 = average volume of a single atom in the crystal, Γ = point impurity scattering parameter,⁴ and v = average sound velocity. These two additional scattering mechanisms have been put into Eq. (2) with

$$\tau_e^{-1} = \tau_b^{-1} + \tau_i^{-1} + \tau_u^{-1}, \quad (7)$$

and K' has been computed for chemically pure CdTe. The numerical constants used for CdTe are given in Tables I and IV. A total of three different theoretical curves, shown in Fig. 7, were calculated. Curve *A* was computed for chemically pure CdTe made of a single isotope each of Cd and Te by setting both τ_b and $\tau_i = \infty$ in Eq. (7). A value of $b=3.0$ was used in τ_u . The calculations for the second curve, *B*, included τ_b , τ_i , and τ_u with $b=3.0$, $p=7.02 \times 10^{-16} \text{ sec}^{-1}$. For the third curve, curve *C*, τ_u was changed somewhat by making $b=4.5$ and $p=6.28 \times 10^{-16} \text{ sec}^{-1}$, but τ_b and τ_i were left unchanged. In all cases the value of p was obtained

⁵¹ D. K. C. MacDonald and L. T. Towle, Can. J. Phys. **34**, 318 (1956).

⁵² B. Abeles, Bull. Am. Phys. Soc. **8**, 14 (1963).

⁵³ P. G. Klemens, Proc. Phys. Soc. (London) **A68**, 1113-28 (1955).

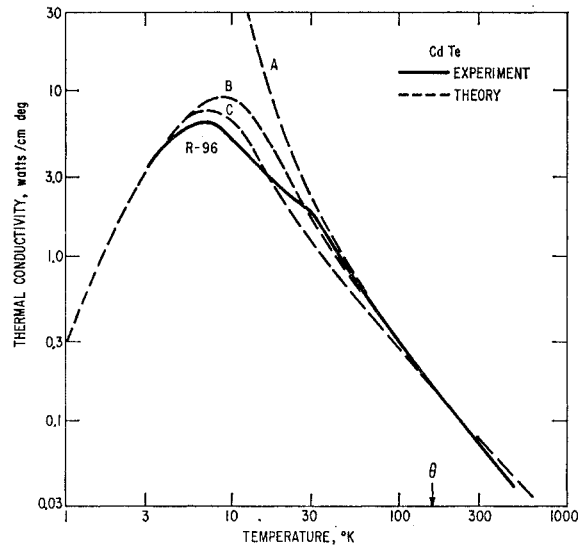


Fig. 7. Theoretical and experimental curves of the thermal conductivity of pure CdTe versus temperature. The heat is transported by phonons which are scattered by various processes. Curve *A* assumes only umklapp scattering is present, and that the exponential factor $b=3.0$. Curve *B* assumes that boundary, isotope, and umklapp scattering are present and $b=3.0$. Curve *C* assumes the same three mechanisms as in curve *B*, but now $b=4.5$.

by fitting the computed curve to the experimental curve at $T=\theta$.

The physical properties of CdTe in Table IV need some explanation. The elastic constants c_{ij} are those given by McSkimin and Thomas⁵⁴ at 298°K. The value of $\theta=158^\circ\text{K}$ has been computed for $T=0^\circ\text{K}$ using these c_{ij} values.⁵⁵ If true c_{ij} values for 0°K had been available, the computed θ might have been 160 to 165°K. Such a change in θ would make no significant difference in K' . An approximate value⁵⁶ of $\theta=200^\circ\text{K}$ for CdTe has been obtained from specific heat measurements at 80°K. The value of $\theta=158^\circ\text{K}$ is preferred since it is more in line with the trend in θ values for the elements and compounds in the fifth row of the periodic table. For example grey tin^{57,58} has $\theta=212^\circ\text{K}$, indium antimonide^{56,58,59} has $\theta=205^\circ\text{K}$, and rubidium iodide⁶⁰ has $\theta=102^\circ\text{K}$. The average sound velocity, v , has been computed from ρ and the c_{ij} values. The point-defect scattering parameters Γ have been computed from the isotope masses and their natural abundances.⁶¹

The general shape of the experimental K versus T curve for R-96 is reproduced with $b=3$ and the normal

⁵⁴ H. J. McSkimin and D. G. Thomas, J. Appl. Phys. **33**, 56 (1962).

⁵⁵ J. deLaunay, J. Chem. Phys. **22**, 1676 (1954).

⁵⁶ P. V. Gulyaev and A. V. Petrov, Fiz. Tverd. Tela **1**, 368 (1959) [translation: Soviet Phys.—Solid State **1**, 330 (1959)].

⁵⁷ F. J. Webb and J. Wilks, Proc. Roy. Soc. (London) **A230**, 549 (1955).

⁵⁸ J. C. Phillips, Phys. Rev. **113**, 147 (1959).

⁵⁹ L. J. Slutsky and C. W. Garland, Phys. Rev. **113**, 167 (1959).

⁶⁰ S. K. Joshi and S. S. Mitra, Proc. Phys. Soc. (London) **76**, 295 (1960).

⁶¹ D. Strominger, J. M. Hollander, and G. T. Seaborg, Rev. Mod. Phys. **39**, 585 (1958).

isotopic abundance, i.e., curve *B*, except that some additional phonon scattering above that caused by boundaries, isotopes, and umklapp processes appears to be present in the CdTe samples for $7^\circ\text{K} < T < 30^\circ\text{K}$. The theory may give too high a *K* between 7 and 30°K because we have neglected some intrinsic feature of CdTe or else we have not included the phonon scattering produced by some type of crystal imperfection. Possible intrinsic troubles with the theory might be an incorrect τ_u , the neglect of dispersion in the phonon spectrum, the failure to include normal phonon processes along with the isotope scattering,⁴² or perhaps the failure to separate the phonons into longitudinal and transverse branches.⁴⁰

It is also possible that some chemical impurity is responsible for this increased phonon scattering and for the noticeable change in slope of *K* versus *T* at 30°K . Curves of *K* versus *T* of a similar nature have been seen⁶² for silicon crystals containing about $1 \times 10^{18} \text{ cm}^{-3}$ of oxygen. Just what impurity in CdTe could cause this behavior is not clear. The oxygen content of *R-96* was measured with a mass spectrometer as $5 \times 10^{16} \text{ cm}^{-3}$. At this low a concentration oxygen, which should substitute for tellurium, is obviously not the cause. From Table II one might be led to suspect C, Si, Li, or some other unlisted element. More work will be needed to explain this discrepancy between 7 and 30°K in CdTe.

In the so-called boundary scattering region below 7°K the observed *K* for *R-96* agrees quite well with the value calculated from a combination of diffuse boundary scattering and isotope scattering, see Fig. 7. If this boundary scattering curve is calculated for crystal *R-69*, see Fig. 1, the calculated value is 3 times greater than the observed one at 3°K . The calculated value at 3°K for *R-85* in Fig. 1 is 50 times greater than observed. Residual impurities and/or deviations from stoichiometry are responsible for these *K* values begin lower than the boundary scattering limit. However, the results for *R-96* show that it is possible to make CdTe crystals which do come quite close to the theoretical predictions. Thus, it is now possible to proceed to the study of the effects of intentionally added impurities on the *K* of CdTe.

Doped CdTe

The *K* of the Zn-doped CdTe is the easiest to understand in terms of the theory of phonon scattering by point defects. Since Zn is nonmagnetic, it will scatter essentially like a mass defect in the lattice. The Γ value for the mass fluctuation scattering by the Zn is computed on the assumption that the Zn atoms substitute for Cd atom in a random fashion.¹⁵ The result (see Table IV) is $\Gamma(\text{Zn}_{0.01}\text{Cd}_{0.99}\text{Te}) = 9.37 \times 10^{-5}$. The intro-

duction of the Zn actually distorts the lattice and changes the interatomic bonding around its lattice site. Hence, the over-all scattering cross section of the Zn will be larger than that given above.⁵⁵ In order to fit the *K* curve for the Zn-doped sample in Fig. 4, it is necessary to use an equivalent value of Γ in Eq. (2) and (6) which is about 5 times 9.37×10^{-5} . Thus, the Zn is about 5 times as effective a scatterer as one would calculate simply on the basis of its mass difference. Thus, the total scattering number, S^2 in Klemen's⁵³ notation, has a not unreasonable value of $S^2 \approx 0.1$ for Zn in CdTe. This point-defect scattering combined with the umklapp and boundary scattering that was employed for pure CdTe gives a reasonable fit to the Zn-doped curve shown in Fig. 4. This crystal has been heat treated in Cd vapor, and there is no need to include an extra phonon scattering mechanism in the so-called boundary scattering region below 7°K . Such a mechanism is necessary to explain the results in the untreated crystal, *R-72*.

The *K* curve for the Mn-doped CdTe crystal, *R-94*, in which 1% of the Cd has been replaced by Mn, is very nearly the same as that for the 1% Zn sample from 10 to 300°K . This means that for these temperatures the scattering cross sections of Mn and Zn are the same. This near equality of cross section indicates that Mn is behaving like a nonmagnetic impurity, and shows no magnetic scattering between 10 and 300°K . In the temperature region below 10°K the *K* of *R-94* in Fig. 4 is 75% of that of the Zn-doped sample. It appears that the Mn-doped crystal, after heat treatment in Cd vapor, is not quite as close to being stoichiometrically perfect as is the Zn-doped crystal. This small difference is negligible for the present purposes. The phonon scattering produced by the magnetic Mn atoms is almost identical with that produced by the nonmagnetic Zn atoms. This behavior is in sharp contrast to that of the Fe atoms.

The Fe-doped crystal in Fig. 4 has a *K* noticeably lower than the Zn- or Mn-doped crystals over the whole range from 3 to 100°K . At 300°K the three different impurities, Zn, Mn, Fe, all have nearly the same small effect on the *K* of CdTe. Since the Mn and the Zn behave like nonmagnetic impurities, the problem is how to account for the possible magnetic scattering which is producing the low *K* of the Fe-doped CdTe between 3 and 100°K .

MAGNETIC SCATTERING

Energy Levels

The rather large phonon scattering cross section of the Fe ions in the CdTe between 3 and 100°K is believed to depend on their magnetic nature. Thus, it is necessary to know the position of the Fe in the CdTe lattice. From paramagnetic resonance data on a large number of II-VI compounds Ludwig and Woodbury⁶³ state that as

⁶² M. G. Holland, *Proceedings of the International Conference on Semiconductor Physics, Prague, 1960* (Czechoslovak Academy of Science, Prague, 1961 and Academic Press Inc., New York, 1962), p. 633.

⁶³ G. W. Ludwig and H. H. Woodbury in *Solid State Physics*,

far as is known the transition metals, M , always substitute for the Cd (or the Zn). These authors further find that interstitial M ions appear to occur, so far, only in silicon. To date, the three elements Cr, Mn, and Co have been seen^{63,64} to be substitutional impurities in CdTe. Optical absorption data⁶⁵ for Fe, Co, Ni, and Cu in CdS indicate that these elements are in a tetrahedral environment. Paramagnetic resonance studies⁶⁶ of Fe in CdS show that the Fe does not normally have a d^5 configuration (i.e., Fe^{3+}), but can be changed to this configuration at low temperatures by optical excitation. From measurements of the paramagnetic resonance of Fe-doped CdTe, Castner⁶⁷ has concluded that the Fe does not normally have a d^5 configuration in this crystal either.

From these several observations it seems that the most reasonable position for the Fe is as a substitute for a Cd atom, and therefore, is in a tetrahedral environment. Its nominal charge state on an ionic model is Fe^{+2} , which implies a d^6 configuration. It is also possible, though not likely, that the Fe acts as an acceptor and is nominally Fe^{+1} at low temperatures, or d^7 . The Mn almost certainly⁶⁸ replaces the Cd, and has a Mn^{2+} , d^5 configuration. The Zn impurities also substitute¹⁵ for the Cd.

The Mn^{2+} , d^5 ions in the Cd sites have a 6S ground state. This 6S state is split into a series of 6 substates by the hyperfine interaction⁶⁸ of the d electrons with the nuclear magnetic moment of the Mn^{55} . The highest energy level of these substates lies at an energy⁶⁹ of $15A = 0.0825 \text{ cm}^{-1}$ or 0.119°K above the ground state. These hyperfine energy levels are further split into 36 levels by the cubic crystalline electric field. This splitting of each hyperfine level amounts to an energy⁶⁹ of about $3a = 0.0084 \text{ cm}^{-1}$, an effect only 10% as large as that caused by the hyperfine interaction. Thus, the atomic 6S ground state of the Mn, d^5 ion is split into a number of energy levels, the highest level lies at an energy kT above the ground state, where this equivalent temperature $T \approx 0.1^\circ\text{K}$. In Mn, d^5 the next atomic level above the 6S state is a 4G state.⁷⁰ In a crystalline field of $Dq \approx 400 \text{ cm}^{-1}$, a reasonable value for Mn, d^5 in a tetrahedral environment, the 4G state gives rise to a substate level at an energy of about $24\,000 \text{ cm}^{-1}$ or $3.5 \times 10^4^\circ\text{K}$ above the 6S state. These various energy levels shown in Fig. 8(a) are all given for zero-magnetic field. The main feature of these levels for Mn in CdTe is that they are at energies either much greater than or

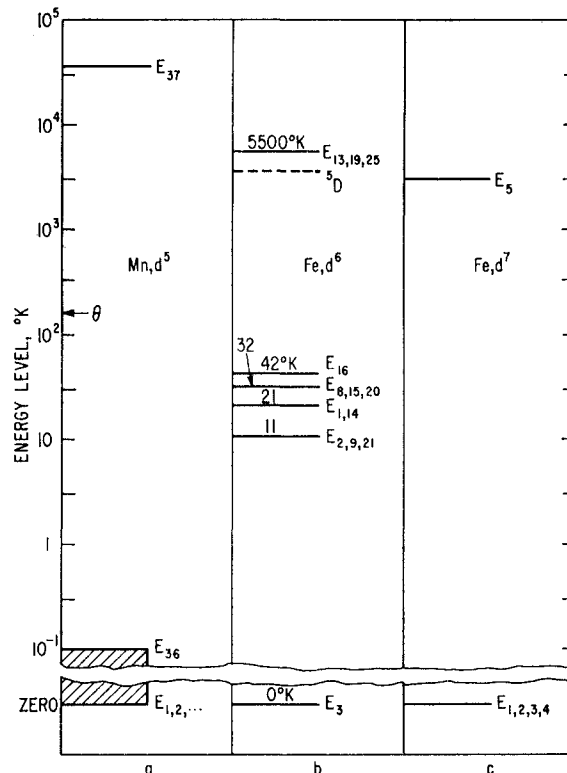


FIG. 8. The energy levels for various transition-metal ions in a tetrahedral Cd lattice site in CdTe. The energies, kT , are given in terms of the temperature, T . Note the change from a linear to a logarithmic scale just above zero. In (a) the low-lying nearly degenerate ground state of Mn, d^5 with levels $E_1 \dots E_{36}$ is derived from the free-ion 6S state. The first excited level at $\sim 35\,000^\circ\text{K}$ comes from the 4G free-ion state. In (b) all of the levels shown for the Fe, d^6 are derived from the 5D free-ion state (shown as a dashed line). The levels between 0 and 42°K come from the orbital doublet 5E . The level at 5500°K comes from the orbital triplet 5T_2 . In (c) a scheme is given for the hypothetical Fe, d^7 configuration. All the levels come from the free-ion 4F state. The degenerate ground state is an orbital singlet 4A_2 , while the level at approximately 3000°K comes from the orbital triplet 4T_2 .

much less than the phonon energies in the 3 to 300°K measurement range.

The situation for Fe in CdTe is rather different. First consider the case where the Fe has a d^6 configuration. This energy level scheme has been worked out by Low and Weger.⁷¹ In their notation the spin-orbit coupling parameter, λ , is negative and is approximately $\lambda \approx -100 \text{ cm}^{-1}$. The crystal field parameter, Dq , is positive for a tetrahedral site and might be similar to the value of $Dq \approx +350 \text{ cm}^{-1}$ found for Fe^{2+} in ZnS. Somewhat different values could be used for λ and Dq . The free-ion value^{72,73} of λ for Fe^{2+} , d^6 , 5D ground state is -101 cm^{-1} . The value for the ion in the solid is probably about 70% of this, or -70 cm^{-1} . Some measurements by

edited by F. Seitz and D. Turnbull (Academic Press Inc., New York, 1962), Vol. 13, p. 223; also see p. 295.

⁶⁴ G. W. Ludwig and M. R. Lorenz (to be published).

⁶⁵ R. Pappalardo and R. E. Dietz, Phys. Rev. 123, 1188 (1961).

⁶⁶ J. Lambe, J. Baker, and C. Kikuchi, Phys. Rev. Letters, 3, 270 (1959).

⁶⁷ T. G. Castner (private communication).

⁶⁸ J. S. Griffith, *The Theory of Transition-Metal Ions* (Cambridge University Press, Cambridge, England, 1961), p. 115.

⁶⁹ J. Lambe and C. Kikuchi, Phys. Rev. 119, 1256 (1960).

⁷⁰ L. E. Orgel, J. Chem. Phys. 23, 1004 (1955).

⁷¹ W. Low and M. Weger, Phys. Rev. 118, 1119 (1960).

⁷² D. S. McClure, in *Solid State Physics*, edited by F. Seitz and D. Turnbull (Academic Press Inc., New York, 1959), Vol. 9, p. 399; also see pp. 426-428.

⁷³ Ref. 68, p. 111.

the present authors on the optical absorption of FeAl_2O_4 , where Fe^{+2} is in a tetrahedron of oxygen ions, give $Dq = +400 \text{ cm}^{-1}$. McClure⁷² gives $Dq = -1000 \text{ cm}^{-1}$ for Fe^{+2} octahedrally coordinated by H_2O . In MgO divalent Fe has⁷⁴ a value of $Dq = -1030 \text{ cm}^{-1}$. A tetrahedral site should have a $Dq = (4/9) \times 1015 \text{ cm}^{-1} = 450 \text{ cm}^{-1}$. Thus, we shall assume a not unreasonable value of $Dq = +400 \text{ cm}^{-1}$ for Fe, d^6 in CdTe. The energy levels for this d^6 configuration in a tetrahedral site are shown in Fig. 8(b). Here the energies, again for zero-magnetic field, are converted to equivalent temperatures. The E_i designations are those used by Low and Weger. The number of separate E_i designations on a particular level indicates its degeneracy. The eigenfunctions of these substates are composed of a combination of orbit plus spin-wave functions, and are tabulated.⁷¹ The ground state, E_3 , is a singlet with no degeneracies. There are four low-lying excited states at temperatures of 11, 21, 32, and 42°K . The fifth excited state occurs at a very high energy equivalent to 5500°K . There are others at still higher energies. The dashed line in Fig. 8(b) indicates the energy of the original, 25 fold degenerate, free ion 5D state from which the present series of substates was derived.

It is also possible that the Fe in the CdTe acts as an electron acceptor, and occurs in the unusual Fe^{+1} charge state with a d^7 configuration. Such a charge state has been seen⁷⁵ for Fe in NaF. The energy level scheme for d^7 in a tetrahedral field has been given by Orgel.⁷⁰ The ground state is 4A_2 , which is an orbital singlet with a four-fold spin degeneracy. This spin degeneracy is not split in a strictly cubic field, but can be split by hyperfine interactions, or distortions from a strictly cubic field.⁷⁶ The hyperfine interaction with the Fe would occur only for Fe^{57} , which is the only isotope with a nonzero nuclear magnetic moment. However, Fe^{57} has a natural abundance of only 2.2%, and a very small nuclear moment. Hence, the ground state of Fe, d^7 is essentially not split by hyperfine interactions. There may be noncubic distortions of the crystalline field around these Fe sites in CdTe caused by local strains, nearby vacancies, dislocations, etc. These effects are difficult to evaluate, but they would probably produce a ground-state splitting of only a fraction of 1°K . This energy level scheme for Fe, d^7 is shown in Fig. 8(c). The E_i levels indicate the degeneracy, but are otherwise labeled arbitrarily.

Other configurations for the Fe in the CdTe can be imagined, but the most likely ones of d^5 , d^6 , or d^7 in a tetrahedral crystalline field have been enumerated. The occurrence of d^5 has been ruled out by the electron paramagnetic resonance measurements leaving d^6 and d^7 as possibilities. The manner in which phonons can

interact with these two configurations is the next problem.

Phonon Interactions

There are certain energy requirements and selection rules governing the scattering of phonons by their interaction with magnetic impurity ions. Some of these rules have been discussed by Orbach *et al.*,^{77,78} Seiden,⁷⁹ Mattuck and Strandberg,⁸⁰ and Van Vleck.⁸¹

The first consideration is the relation between the phonon energy and the energy separation between two energy levels of the magnetic ion. If the phonon energy is equal to the level separation, then the phonon can be absorbed and a second phonon of the same energy is later emitted. This is the so-called direct scattering process. A second process is the "Raman" process in which the difference in energy between the incoming and outgoing phonons is equal to the separation between two magnetic levels. If the level separation is greater than the phonon energy, no scattering will take place. When both direct and Raman processes are possible, the direct processes will be dominant, and hence will determine K . The phonons that are most important in determining K in a Debye-type solid have an energy of $3.9 kT$ or $k\theta$, whichever is smaller. This phonon cutoff at $k\theta$ means that in CdTe we do not have to consider any magnetic energy levels above 158°K , see Fig. 8.

When the phonon energy matches the level separation the phonon can be absorbed. The absorption probability depends upon the matrix element between the two states. The mechanism of the phonon-magnetic moment interaction is as follows. The phonon waves passing a magnetic cation in the lattice will alter the positions of the four anions which surround the cation. This will cause distortions in the crystalline field at the cation, and alter the relative energies of the various orbital wave functions. This mechanism is known as the orbit-lattice interaction. There is no direct interaction between the phonons and the spins of the individual d -shell electrons. Any spin-phonon interaction comes about in second order through the spin-orbit coupling parameter, λ . From this discussion, we see that those levels which are spin-only levels, such as those derived from the 6S free-ion state of Mn^{2+} (or Fe^{3+}) will be very weakly⁷⁸ coupled to the phonons. Experimentally, we are concerned with phonons of energies, kT , from about 1 to 158°K . Thus, the very low-lying energy levels shown in Fig. 8(a) for Mn^{2+} , d^5 can only scatter these phonons by Raman processes. Since this scattering will also be weak, the Mn^{2+} impurities should have very

⁷⁷ R. Orbach, *Phil. Mag.* **5**, 1303 (1960); *Phys. Rev. Letters* **8**, 393 (1962); *Phys. Letters* **3**, 269 (1963).

⁷⁸ M. Blume and R. Orbach, *Phys. Rev.* **127**, 1587 (1962).

⁷⁹ J. Seiden, *Compt. Rend.* **254**, 3653 (1962).

⁸⁰ R. D. Mattuck and M. W. P. Strandberg, *Phys. Rev.* **119**, 1204 (1960).

⁸¹ J. H. Van Vleck, *Phys. Rev.* **57**, 426 (1940).

⁷⁴ W. Low and M. Weger, *Phys. Rev.* **118**, 1130 (1960).

⁷⁵ B. Bleaney and W. Hayes, *Proc. Phys. Soc. (London)*, **B70**, 626 (1957).

⁷⁶ F. S. Ham, G. W. Ludwig, G. D. Watkins, and H. H. Woodbury, *Phys. Rev. Letters* **5**, 468 (1960).

little effect on the K of CdTe. Experimentally we see that Zn^{+2} and Mn^{+2} behave similarly. The main phonon scattering is of a point-impurity type caused by mass defects and local lattice strains.

An ion with a d^7 configuration, such as Fe^{+1} would have, possesses an orbital singlet ground state which is four-fold spin degenerate, see Fig. 8(c). Because the phonon-spin interaction is very small, and there are no levels within $158^\circ K$ of the ground state E_1 , the phonon scattering by a d^7 ion should be extremely small. The only scattering possible might be a Raman scattering between some of the E_1, E_2, E_3, E_4 , levels which have been slightly separated by local lattice strains.⁸² This scattering and that due to Mn, d^5 might show up at temperatures below $0.1^\circ K$ where the phonon energies would be comparable to the splittings.

We shall now consider the phonon scattering from the d^6 configuration. Its scattering should be very small at temperatures much below $2.8^\circ K$ and much above $42^\circ K$, but should be quite large between these two temperatures. Both the d^5 and d^7 configurations are of the Kramer's type in that they have an odd number of electrons and a degenerate ground state. The d^6 configuration has an even number of electrons, and as Fig. 8(b) shows, its ground state is nondegenerate. The next higher level, E_2 etc., is at $11^\circ K$. Thus, for low temperatures $3.9T < 11^\circ K$, i.e., $T < 2.8^\circ K$, when the dominant phonons have energies less than $11^\circ K$, there should be very little phonon scattering. The scattering should disappear rapidly at temperatures much below $2.8^\circ K$, and K will then be determined by boundary scattering. This type of behavior seems to occur in $R-70$, see Fig. 4, where the K of the Fe-doped sample is approaching that of the Zn-doped CdTe. Their K curves might "meet" at $\sim 1^\circ K$. For temperatures between about 2.8 and $42^\circ K$, the energy of E_{16} in Fig. 8(b), there will be many coincidences between the phonon energies and the level separations for the d^6 configuration. The eigenfunctions of the levels between 0 and $42^\circ K$ all contain substantial orbital contributions, as shown by Low and Weger. This means that the phonon coupling to them via the orbit-lattice interaction is strong, and the scattering should be large. A calculation of the phonon-scattering cross section will be difficult because there are 5 different levels, and transitions are possible not only from the ground state to the higher levels but also between the higher levels themselves. However, some general statements can be made. For example, the phonon scattering will increase with increasing T for $T > 2.8^\circ K$ because more and more of the higher levels become involved in the transitions. The phonon mean-free path should decrease with increasing temperature. Furthermore, the transition probability between two levels will depend on their population differences. Hence, when kT becomes large compared to the level separation, Δ_{ij} , the populations of levels i and j will become nearly equal and the scattering will decrease. So for temperatures much above $42^\circ K$, the phonon scattering by the

d^6 configuration will decrease, and at higher temperatures will be masked by mass-defect and phonon-phonon scattering. This effect can be seen in Fig. 2 for samples $R-70$ and $R-73$ where above $100^\circ K$ the K of these Fe-doped samples is almost the same as the Zn- and Mn-doped ones. Above $300^\circ K$ the K of all the samples is nearly the same as for pure CdTe, and is dominated by phonon-phonon scattering.

In the intermediate temperature range between 2.8 and $50^\circ K$ the shape of the K versus T curves for $R-70$ and $R-73$ indicates that K is varying about as $T^{+0.5}$. In this region the specific heat capacity per unit volume, C , is varying as T^3 to T^2 . The phonon mean-free path, l , can be estimated from Debye's expression

$$l = 3K/vC. \quad (8)$$

This qualitative argument indicates that, between 2.8 and $50^\circ K$, l is decreasing with increasing temperature as

$$l \sim T^{-2} \text{ or } T^{-3}. \quad (9)$$

At $42^\circ K$, where the paramagnetic scattering is about at its strongest, the measured value of $K \approx 0.15$ W/cm deg, and $C = 0.66$ J/cm³ deg. These give $l \approx 340$ Å from Eq. (8). This mean free path and an Fe concentration of 1.6×10^{20} cm⁻³ give an experimental cross section per Fe atom of $18(\text{Å})^2$. Now the dominant phonons at $42^\circ K$ have a wavelength of about a lattice constant, a_0 , or 6.5 Å. These wavelengths are roughly the size of the magnetic ions, so we can say, crudely, that a strong scattering by the magnetic ion would have a scattering cross section of the order of its geometric cross section, $V_0^{2/3}$ (See Table IV), of 10.5 Å². This value is about $\frac{1}{2}$ of the experimental cross section. Even though these numerical arguments are all very rough, it can be concluded that the Fe ions are, as predicted, strong phonon scatterers at $42^\circ K$. It would therefore seem likely that most of the Fe occurs in a d^6 configuration, and little if any in a d^7 .

OTHER K MEASUREMENTS

Some other measurements on the K of crystals containing various transition metal ions have been reported. A short review has been given in Ref. 4 which mentions Fe^{2+} in $MgAl_2O_4$ studied by Slack, Fe^{2+} in $ZnSO_4 \cdot 7H_2O$ studied by Rosenberg and Sujak, Mn^{2+} in $NaCl$ studied by Klein, and Cr^{3+} in Al_2O_3 studied by Berman, Foster, and Rosenberg. There are also some recent studies on V^{3+} and Cr^{3+} in Al_2O_3 by Dreyfus and Zadworny,⁸³ Cr^{3+} in Al_2O_3 by Holland,⁸⁴ and Co^{2+} in $La_2Co_3(NO_3)_{12} \cdot 24H_2O$ by Berman, Brock, and Huntley.⁸⁵ The systems which should show pronounced phonon scattering are those which are nearly orbitally

⁸² W. Low, in *Solid State Physics*, edited by F. Seitz and D. Turnbull (Academic Press Inc., New York, 1960), Suppl. 2, p. 41.

⁸³ B. Dreyfus and F. Zadworny, *J. Phys. Radium*, **23**, 490 (1962).

⁸⁴ M. G. Holland, *J. Appl. Phys.* **33**, 2910 (1962).

⁸⁵ R. Berman, J. C. F. Brock, and D. J. Huntley, *Phys. Letters* **3**, 310 (1962/3).

degenerate in the ground state. Nearly degenerate means having several low-lying (10 to 100°K) levels above the ground state. These would be Fe²⁺ in four-fold, tetrahedral coordination with oxygen in MgAl₂O₄; Fe²⁺ in six-fold, approximately octahedral coordination with H₂O in ZnSO₄·7H₂O; V³⁺ in sixfold, nearly octahedral coordination with oxygen in Al₂O₃; and possibly Co²⁺ in La₂Co₃(NO₃)₁₂·24H₂O. Neither the Mn²⁺ in NaCl (which is an ⁶S state ion) or the Cr³⁺ in Al₂O₃ (which has an orbital singlet ground state) should show a large magnetic scattering of phonons. Of these several systems only Fe²⁺ in MgAl₂O₄, Fe²⁺ in ZnSO₄·7H₂O, and Cr³⁺ in Al₂O₃ have been studied sufficiently and over a large enough temperature range to see the magnetic scattering in zero magnetic field. The scattering cross section of the Fe²⁺ is large in both cases, and that of the Cr³⁺ is small,⁴ as predicted.

ULTRASONIC ATTENUATION

Very little general comparison can be made between the present results and the microwave-phonon attenuation measurements of Shiren⁸⁶ and Tucker.⁸⁷ They have measured the attenuation caused by different paramagnetic impurities in MgO. These results can be correlated with other static data of Watkins and Feher⁸⁸ on the strain-impurity interaction. The microwave results are concerned with the absorption of phonons of about 10¹⁰ cps in degenerate ground-state levels which are split by an applied \bar{H} field. In contrast the thermal phonons with frequencies of about 10¹² cps are absorbed by transitions from the ground state to higher-energy states when $\bar{H}=0$. The absorption processes, as has been shown, depend on the details of the crystalline field at the magnetic ion and on its resultant structure of energy levels. As a rule of thumb it appears that, for a given paramagnetic impurity in a given lattice, a large microwave-phonon absorption and a large scattering cross section for thermal phonons both indicate the existence of some low-lying energy levels a small distance above the ground state.

CONCLUSIONS

1. Mixed crystals of CdTe containing 1 mole % of Mn, Fe, or ZnTe have been grown from the melt. Some of the observed crystal chemistry properties can be understood in terms of the covalent tetrahedral radii of the transition metals. A set of values of such radii for the first transition metal series has been derived.

2. The thermal conductivity, K , of reasonably pure CdTe has been measured from 3 to 300°K, and a table of smoothed values is given. The results can be satisfactorily explained by a simple theory in which phonons transport the heat and are scattered by the crystal boundaries, the natural isotopes, and other phonons.

⁸⁶ N. S. Shiren, *Bull. Am. Phys. Soc.* **7**, 29 (1962).

⁸⁷ E. B. Tucker (private communication).

⁸⁸ G. D. Watkins and E. Feher, *Bull. Am. Phys. Soc.* **7**, 29 (1962).

Between 7 and 30°K the measured K is somewhat less than is predicted by this theory, thus suggesting the presence of a small concentration of an unknown impurity or perhaps an intrinsic scattering mechanism not included in the theory.

3. The K of CdTe doped with nonmagnetic Zn has been measured from 3 to 300°K. These results can be explained by using the theory for pure CdTe with the inclusion of some additional point impurity scattering produced by the Zn.

4. Measurements of the K of crystals of CdTe containing the magnetic ions Mn or Fe have been made over the same temperature range in zero-magnetic field. These results can be explained by some magnetic scattering in addition to that produced by a nonmagnetic Zn-like impurity. This extra magnetic scattering is small or absent in the case of Mn but is quite large for the Fe. This magnetic scattering is explained in terms of the details of the arrangements of the free-ion states of the d -shell electrons as they are split by the crystal-line field and spin-orbit coupling. Qualitative agreement between the predictions of this theory and the experimental results has been found.

APPENDIX: THE DERIVATION OF TETRAHEDRAL RADII

We are interested in determining the ease with which Cd in CdTe can be replaced by the various transition metals in the first transition metal series. CdTe has a zincblende structure and can be visualized as a covalently bonded crystal in which each Cd is surrounded by a tetrahedron of Te atoms. In such an environment the Cd to Te separation can be taken as the sum of the neutral radii of the Cd and the Te atoms. This concept of a neutral covalent radius r_t of an atom in a tetrahedral environment has been described by Pauling.⁸⁹ The radii for the nontransition elements such as Zn, Ga, Ge, As, Se, Br, Ag, Cd, In, Sn, Sb, Te, and I are relatively easy to specify. Values for their r_t have been taken from Table 7-13 of Pauling's book, and are plotted in Fig. 9. In a few cases small changes have been made in Pauling's values to take into account new determinations of the lattice parameters of the crystals. The crystal structures and x-ray lattice parameters used here have been taken from Wyckoff⁹⁰ unless otherwise stated.

The radii of these transition metals will depend upon the number of electrons in their $3d$ shells. This point has been reviewed by Orgel.⁹¹ On an ionic model the formal charge of the Cd in CdTe is Cd²⁺. Thus we shall attempt to determine r_t from those transition-metal compounds where the metal atom has a formal charge of $2+$. This means that we want to know r_t for Fe with a

⁸⁹ L. Pauling, *The Nature of the Chemical Bond* (Cornell University Press, Ithaca, New York, 1960), 3rd ed., Chap. 7.

⁹⁰ R. W. G. Wyckoff, *Crystal Structures* (Interscience Publishers, Inc., New York, 1948-1960).

⁹¹ L. E. Orgel, *An Introduction to Transition-Metal Chemistry* (Methuen and Company, Ltd., London, 1960), p. 69.

d^6 configuration, or Fe^{2+} , but not with a d^5 configuration, or Fe^{3+} . We also want Cu as d^9 but not as d^{10} . In Fig. 9 the r_t values for both d^9 and d^{10} Cu have been plotted for comparison. They are obviously not equal. Similarly we would like to know d^1 Sc, i.e., Sc^{2+} . This charge state is not found experimentally, so that the value in Fig. 9 for Sc is based on Sc^{3+} with some adjustment to yield an approximate value for Sc^{2+} . In some of the compounds, for example FeS_2 , it is difficult to ascertain the d -shell configuration. Therefore, we have generally tried to avoid such compounds in determining the present r_t values.

The first element of interest in the metal series is Ca. The r_t of Ca has been computed from the atomic separations in CaS, CaSe, and CaTe using Pauling's values of 1.04, 1.14, and 1.32 Å for the covalent radii of S, Se, and Te, respectively. These three crystals have a NaCl crystal structure, and yield a value of 1.82 Å for the radius of Ca in a six-fold octahedral coordination. A multiplication factor of 0.90 was used to reduce the octahedral radius to a tetrahedral value of 1.64 Å. This multiplication factor of 0.90 is based on the compounds MnS and MnSe, where Mn(d^5) occurs in an octahedral environment with a 1.58 Å radius in the NaCl-type modifications, and in a tetrahedral environment with a 1.39 Å radius in the zinc-blende and wurtzite modifications. This same factor of 0.90 has been found by Rigamonti²⁰ in comparing tetrahedral and octahedral radii of Mn and Cd in oxides. This octahedral to tetrahedral conversion has also been used in determining the r_t of Ti, V, and Cr from data on their monosulfides, selenides, and tellurides. The tetrahedral radius of 1.32 Å for Fe has been determined directly from the data of Chudoba and MacKowsky¹⁶ on zinc-blende structure mixed crystals of $(Fe_xZn_{1-x})S$ with $x \leq 0.44$, and the Fe-Se (and Fe-Te) separation in tetrahedrally coordinated Fe in α FeSe (and β FeTe). This value of 1.23 Å for Fe is noticeably greater than Pauling's value of 1.11 (1.23 Å octahedral) based on FeS_2 -type crystals containing Fe, and is close to Huggins⁹² value of 1.29 Å. The value of r_t for Co is based on both oxides and sulfides. From mixed crystals of $(Co_xZn_{1-x})O$ studied by Robin²¹ and Rigamonti²⁰ an r_t value of 1.31 Å is computed for Co using an oxygen radius of 0.67 Å. From neutron-scattering data by Roth⁹³ on the normal spinel Co_3O_4 , a radius of 1.27 Å is computed for the tetrahedral site. A radius of 1.28 Å is computed from $CoAl_2O_4$. The x-ray data of Lundquist and Westgren⁹⁴ on the spinel Co_3S_4 ; assumed to be a normal spinel, gives 1.16 Å. The data of Lundquist *et al.*⁹⁵ on Co_9S_8 give 1.10 Å. The Co radius is the most variable one found in the present study. An average r_t

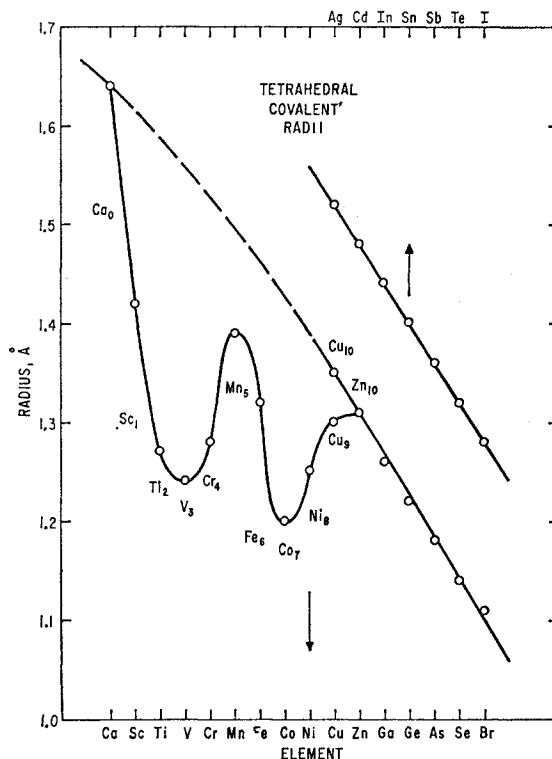


FIG. 9. The covalent, tetrahedral radii of various elements as a function of their atomic number. The various transition metals are assumed to have a "formal charge" of +2. The subscripts on the transition metal series indicate the number of electrons in the $3d$ shell. Thus, the point for Mn_5 is for a d^5 configuration.

of 1.20 Å is taken as representative, and is in good agreement with an octahedral radius of 1.32 Å based on CoS , CoS_2 , $CoSe$, $CoSe_2$, and $CoTe$. The value of 1.23 Å for Ni is based on tetrahedrally coordinated Ni in Ni_3S_2 studied by Westgren,⁹⁶ and three-fold coordinated Ni in NiS and $NiSe$, which both have the millerite structure. The 1.30 Å value for Cu, d^9 , is based on Cu in four-fold coordination in CuO , CuS , $CuSe$, and $CuTe$.

These values for the elements Ca through Cu have been plotted in Fig. 9 along with Pauling's data for the other elements. This graph shows that the transition metals have covalent radii which are noticeably smaller than those of the nontransition metals on either side of them in the Periodic Table. This behavior can also be seen in the metal crystals themselves.⁹⁷ The rather large radius of Mn, d^5 in Fig. 9 has been noted before by Pauling.⁸⁹ Figure 9 shows that Mn^{2+} with a stable half-filled $3d$ shell, approaches the radii (dotted curve) expected for nontransition elements. Manganese is not unique in this respect since both Cr, d^4 and Fe, d^6 exhibit some of this behavior. The minimum radii seem to occur when the d shell is, crudely speaking, $\frac{1}{4}$ or $\frac{3}{4}$ full. A more comprehensive explanation of this effect in terms of the electron occupation of the various orbital

⁹² M. L. Huggins, *Phys. Rev.* **28**, 1086 (1926).

⁹³ W. Roth (private communication).

⁹⁴ D. Lundquist and A. Westgren, *Z. Anorg. Allgem. Chem.* **239**, 85 (1938).

⁹⁵ M. Lindquist, D. Lundquist, and A. Westgren, *Svensk Kem. Tidskr.* **48**, 156 (1936).

⁹⁶ A. Westgren, *Z. Anorg. Allgem. Chem.* **239**, 82 (1938).

⁹⁷ Ref. 89, p. 417.

wave functions is given by Orgel.⁹¹ His analysis would predict that the minima in the curve in Fig. 9 should occur at the d^2 or Ti and the d^7 or Co configurations in a tetrahedral site. The method used here to derive the tetrahedral from the octahedral radii has been crude. Perhaps the relative positions of Ti, and V, derived from octahedral site data, should therefore be reversed.

The main conclusion to be drawn from Fig. 9 is that one should not expect the chemical and crystallographic characteristics of crystals containing transition metals to be a slowly varying function of the atomic number of the transition metal, but will depend critically on the number of electrons in the d shell and on the details of the bonding to the other atoms in the crystal. The solubility of the M atoms in CdTe will,

therefore, vary appreciably as one progresses through the series from Ti to Cu. As shown in the text only part of this series has so far been studied.

ACKNOWLEDGMENTS

The authors would like to thank R. J. Connery for growing the CdTe crystals, and J. H. McTaggart for making the thermal conductivity measurements. They also want to thank M. Lorenz for two pure CdTe crystals and for helpful discussions concerning CdTe. The mass spectrographic results on CdTe have been kindly supplied by H. H. Whitaker of the RCA Laboratories. Thanks are also extended to F. S. Ham and E. B. Tucker for their aid in understanding crystal field theory.